MICROANALYTICAL CHARACTERIZATION OF NORTH DAKOTA FLY ASH

S.A. Benson, D.K. Rindt, G.G. Montgomery, and D.R. Sears

Grand Forks Energy Technology Center
U.S. Department of Energy
Grand Forks, N.D. 58202

INTRODUCTION

Goals of particulate research at the Grand Forks Energy Technology Center (GFETC) include detailed characterization of fly ash with respect to those properties which relate to controlability as well as possible environmental hazards of emissions. The focus is entirely on low-rank western and Gulf Province coals, whose properties are distinctly different from those of eastern coals. Typically the western coals have high moisture, low sulfur, and large variations in the distribution of inorganic constituents.

Beulah, a North Dakota lignite, was used in the combustion tests of primary interest to this paper. This lignite is extraordinarily variable in its inorganic constituents. For example, the sodium content can have a tenfold variation within a few hundred meters in a single seam (1). The specific Beulah lignite used was selected for its high sodium content.

The fly ash was generated for this research using the GFETC Particulate Test Combuster (PTC), illustrated in the schematic in Figure 1. This unit is an axially-fired pulverized coal combustor with a nominal consumption of 34 kg coal/hr. The unit is designed to generate ash characteristic of that produced with similar fuel in a full-sized utility boiler. Axial firing maximizes the fly ash/(bottom ash + slag) ratio. The fly ash samples for analysis were collected at the inlet to the baghouse with two devices, a five-stage multicyclone and a source assessment sampling system (SASS). The flues are equipped with heat exchangers permitting delivery of flue gas to the chosen control device at temperatures from ~100° to 390°C. During these tests, the PTC was equipped with an experimental baghouse because of on-going fabric filter research at GFETC. The PTC instrumentation permits measurement of flue gas condition such as temperature and concentrations of SO_2, NO_x, O_2, and CO_2.

The coal and fly ash were characterized by several analytical techniques. The inorganics of the coal were examined by an extraction technique which selectively removes the inorganics depending upon their association in the coal (2). Low temperature ashing with subsequent x-ray diffraction was used to identify the mineral phases of the coal. The fly ash was examined and analyzed by scanning electron microscope/microprobe, Electron Spectroscopy for Chemical Analysis (ESCA), x-ray diffraction and x-ray fluorescence.

COAL CHARACTERISTICS

The inorganics associated with the Beulah lignite consist of a complex mixture of cations bound to the humic acid groups, possible chelates or coordination complexes, minerals formed during coalification, and minerals accumulated during deposition. Traditional and non-traditional methods were used to examine the coal characteristics. The traditional analysis of the lignite is summarized in Table 1 which lists the ultimate analysis, moisture, heating value, and major element ash analysis.

One of the two "non-traditional methods" used is low-temperature ashing in an oxygen plasma at 150°C with x-ray diffraction analysis to determine the crystaline phases in the ash. The phases identified include SiO_2 (quartz), FeS_2 (pyrite), kaolinite, and $CaCO_3$ (calcite). The second method involves a procedure which selectively removes inorganics (2). The ion-exchangeable cations and soluble salts are removed with 1M ammonium acetate. The coal is then extracted with 1M hydrochloric acid to remove chelated species, acid decomposible minerals such as carbonates, and oxides. The inorganics remaining in the coal can include FeS_2, organically bound sulfur, quartz, and clay minerals. The elements found to be extracted with ammonium acetate are Na (100% of the total Na content), Mg (88%), Ca (41%), and K (57%). The elements removed by HCl are Mg (20%), Al (61%), Ca (50%) and Fe (30%). The elements which remain are Si (100%), Fe (70%), Al (40%), and S (100%). Table 2 summarizes a study of the inorganic constituents in Beulah lignite and the geologic formation it is found in.

TABLE 1. TYPICAL COAL AND COAL ASH ANALYSIS OF BEULAH, N.D. LIGNITE

Ultimate Analysis, as Fired		Coal Ash Analysis, Percent	
Carbon	46.29%	SiO_2	22.3
Hydrogen	5.29	Al_2O_3	11.7
Nitrogen	.62	Fe_2O_3	9.8
Sulfur	.99	TiO_2	0.9
Ash	8.2	CaO	15.7
Moisture	27.2	MgO	5.3
Heating value	17,460 J/g	Na_2O	9.9
(7512 Btu/lb)		K_2O	0.7
		SO_3	23.0

ASH SAMPLING

Fly ash is sampled isokinetically in three ways in the PTC: 1) Using a modified U.S. EPA "method 5" (3) dust loading filters; 2) by collection in a Southern Research Institute* 5-stage multicyclone which simultaneously samples isokinetically and size fractionates the ash (4,5); 3) by collection in a three-stage cyclone module of an Acurex* Source Assessment sampling system or "SASS-Train" (6,7). Nominal aerodynamic size ranges for the multicyclone and the SASS-Train, at the stated flow rates, appear in Table 3. Nominal size ranges, expressed as aerodynamic diameters in µm are those corresponding to actual flow rates employed. The figures represent the mass median diameters (D_{50}) or "cut points", of the size distribution entering or leaving the stage.

University of Washington Mark III* cascade impactors were used to more precisely determine particle size distribution (7). The cumulative particle size distribution, expressed in aerodynamic diameters, appears in Figure 2. This data is used only for comparison. The bulk of the characterization work was done on the multicyclone and SASS Train samples because the masses of particles collected by the impactor are very small and inadequate for analysis.

*Reference to specific brand names and models is done to facilitate understanding and neither constitutes nor implies endorsement by the Department of Energy.

TABLE 2. INORGANIC CONSTITUENTS IN BEULAH LIGNITE AND SENTINEL BUTTE FORMATION (2)

	Beulah Lignite		Sentinel Butte Formation		
Constituent	Whole Coal	Sink Fraction	Overburden	Lignite	Underclay
Alkali feldspars	XXX		XX	X	X
Augite				X	
Barute	X			X	
Biotite	X		X		
Calcite/dolomite	X	XX	XX	X	
Chlorite			XX	X	X
Galena	X				
Gypsum		XX		XXX	
Hematite		X		XX	
Hornblende			X		
Illite	XXX		XX	X	X
Kaolinte	XXX	X	XX	XXX	XXX
Magnetite	X				
Montmorillonite			XXX	X	XXX
Muscovite	X				
Plagioclase		X	XXX	X	X
Pyrite	XXX	XXX		XX	
Quartz	XXX	XXX	XXX	XXX	XXX
Rutile	X				
Volcanic glass			X		

XXX Abundant
XX Common
X Minor

TABLE 3. AERODYNAMIC SIZE RANGES (UPPER AND LOWER D_{50} CUT POINTS) AND SAMPLE FLOW RATES OF GFETC'S ASH SAMPLING EQUIPMENT

Instrument	Southern Research Institute Multicyclone					Acurex/Aerotherm SASS Train*		
Flow rate employed STD l/min	9.36					113.2		
Stage No.	1	2	3	4	5	1	2	3
Nominal size range (upper and lower D_{50}), µm	>10.3	10.3-5.6	5.6-4.15	4.15-1.9	1.9-1.55	>10	10-3	3-1

RESULTS AND DISCUSSION

Fly ash samples were collected by the SASS Train to provide larger masses but only 3 size cuts for x-ray fluorescence (XRF) and x-ray diffractions (XRD). The elemental trends determined by XRF analysis show increasing concentration of Na_2O and SO_3 and decreasing SiO_2, CaO, Fe_2O_3, and MgO with decreasing particle size. Very little change was noted for Al_2O_3 or the minor elements (TiO_2, K_2O, and P_2O_5). These relationships are illustrated graphically in Figure 3. X-ray diffraction was used to identify the crystalline species in each size fraction. The trends show the following relationships.

1. Na_2SO_4, $Na_2Ca(SO_4)_2$ are present in the smaller size fractions.
2. SiO_2, CaO noted in larger size fractions and not in smaller size fractions. Fe_3O_4-$MgFe_2O_4$-MgO phases decrease from larger to smaller size fractions.
3. Possible Al_2SiO_5 and K_2SO_4 phases noted in smallest size fractions.

These two bulk particle characterization methods show the trends of the elemental distribution versus particle size and how the elements are combined. The most interesting trend is the increasing amount of Na_2O and SO_3 with decreasing particle sizes. This leads to the particle-to-particle characterization using the scanning electron microscope/microprobe for various sizes of particles collected with the 5-stage multicyclone.

The scanning electron microscope (SEM) equipped with an energy dispersive x-ray analyzer was used to image and analyze particles down to ~1µm in size. The particles were selected at random for analysis by using a grid overlay of points generated by random numbers on the SEM photomicrograph. A typical SEM photomicrograph is shown in Figure 4. One hundred particles for each stage were analyzed, determining 10 elements per particle, and sized. All data was entered into a computing system for correlation analysis.

The average particle size determined from the SEM photomicrographs for each stage are listed in Table 4. Table 4 also lists the Na_2O and SO_3 concentration averages for all five stages along with the ratio of Na_2O to SO_3. The concentrations of Na_2O and SO_3 increase as particle decreases and the ratio of Na_2O to SO_3 is very close to that of pure Na_2SO_4 for stages 1, 3, and 4. The particles collected in stage 5 are not consistent with the other stages in particle-size or in the ratio of Na_2O to SO_3. The reason for the inconsistence in the ratio could be due to the bimodal distribution of SO_3 shown in Figure 5, and also to the presence of $Na_2Ca(SO_4)_2$ noted by XRD in the small size fraction of the SASS samples.

The compositional relationships can be represented by plots of composition versus composition for selected constituent pairs. These plots can be used to ascertain the origin of certain species from the original mineral matter of the coal and the interactions that have occurred during combustion. For example, Figure 6 illustrates the compositional plots for several combinations. Figure 6-1 represents the plot of Al_2O_3 versus SiO_2 which reveals a cluster of points around a slope of approximately 0.8. Minerals having been identified in Beulah (2) include biotite, kaolinite, muscovite, and illite, where the Al/Si ratio is in the range of 0.67-1.0. From this it can be suggested that the alumino-silicate framework remains intact after combustion. The common clay minerals have a range in composition of 25-45% Al_2O_3 and 35-50% SiO_2. Since most of the particles in Figure 6-1 contain less than these percentages, either the aluminosilicates somehow became combined with additional elements or became coated.

The plot of Na_2O versus CaO in Figure 6-2 shows inverse relationship which is supported by the XRF data in Figure 3.

In the plots of SiO_2 versus SO_3 and Al_2O_3 versus SO_3, Figures 6-3 and 6-4, there is a crude negative correlation between SiO_2 or Al_2O_3 and SO_3. Despite considerable scatter, many of the points lie in the region along lines connecting clay minerals, at 0% SO_3, with Na_2SO_4 or glauberite at 0% SiO_2. This is consistent with clay-like particles becoming coated with Na_2SO_4.

TABLE 4. SIZE, SODIUM, AND SULFUR RELATIONSHIPS FOR EACH STAGE OF THE MULTICYCLONE

	Weight Average			
Stage	Particle Size, μm	Na_2O, %	SO_3, %	Na_2O/SO_3
1	5.48	8.60	10.98	0.79
2	1.99	10.78	12.53	0.86
3	1.29	13.20	17.02	0.78
4	1.20	13.98	19.43	0.72
5	1.38	14.99	23.05	0.65

Na_2O/SO_3 in pure Na_2SO_4 = 0.78

Surface analysis of the particles was performed utilizing ESCA. The ESCA analysis technique analyzes to a depth of 20 to 30A. A typical ESCA scan is shown in Figure 7 for Stage 5 particles. The major constituents found on the surface include Ba, O, Ca, Na, C, S, and Si. The published binding energies (8) of the elements detected by the detailed ESCA scans show that Na, Ca, and Ba are present as sulfates. The Na, Al, and Si may be tied up as silicates, but detailed binding energies for such compounds are unavailable in the literature.

The surfaces of the particles were characterized by a sputter-etching technique used to remove surface layers followed by subsequent ESCA analysis. It was found that carbon and sulfur were concentrated on the surface of all five stages of the multicyclone samples. Contamination of the surface of the particles can largely be attributed to the high concentration of carbon. The presence of sodium was noted on the surface of the larger particles but in the smaller size fractions (<1.5 μm) the sodium concentration was more uniform throughout the depth analyzed by sputtering Campbell and others (9) also showed that Na, S, and C were found on the surface of ash particles. In all cases, except for Stage 5, Ca, Al, and Si were found to increase after sputtering.

CONCLUSIONS

The most significant trend noted by all techniques was the increase of sodium and sulfur with decreasing particle size. The relatively more volatile sodium salts may sublimate to form very small particles of pure salt or they may condense on the surfaces of other particles such as aluminosilicates originating from clay minerals of the coal. The latter is supported by the results of the SEM data in Figures 6-3 and 6-4 and the ESCA results. These results support the validity of vaporization-condensation mechanisms of particulate formation. A summary of the possible mechanisms of particulate formation are described by Damle and others (10).

The work described here is part of an ongoing project at GFETC to develop a model for ash formation during the combustion of low-rank coals.

ACKNOWLEDGMENTS

The authors would like to thank Robin Roaldson for his assistance in analyzing particles with the scanning electron microscope and Harold Schobert for his helpful comments in preparation of this paper.

REFERENCES

1. S.A. Cooley, R.C. Ellman, "Analysis of the Northern Grest Plains Province lignites and subbituminous coals and their ash", U.S. Dept. of Energy DOE/GFETC/ RO-81/2, July 1981.

2. H.H. Schobert, S.A. Benson, M.L. Jones, and F.R. Karner, "Studies in the characterization of United States low-rank coals", Proceedings, International Conference on Coal Science, Dussledorf, Sept 1981, p.10-15.

3. "Method 5-determination of particle emission from stationary sources", Code of Federal Regulators, Title 40 Part 60, Appendix A, July 1, 1979 pp 143.

4. W.B. Smith, R.R. Wilson, Jr., and R.B. Harris, "A five stage cyclone system for in situ sampling", Environmental Science and Technology, 13, 1387, (1979).

5. W.O. Lipscomb, "Survey of particulate emissions macro- and micro-sampling and sizing methods and real-time monitoring and sizing methods", U.S. Department of Energy, DOE/FC/10193-T1, February, 1981.

6. D.E. Blake, "Source Assessment Sampling System: Design and Development", U.S. Environmental Protection Agency EPA-600/7-78-018, February, 1978.

7. W.B. Smith, P.R. Cavanaugh, and R.R. Wilson, Technical Manual: A Survey of equipment and methods for particulate sampling in industrial process streams. U.S. Environmental Protection Agency, Research Triangle Park, N.C. EPA-600/7-78-043 March, 1978.

8. Handbook of X-ray photoelectron spectroscopy, Perkin-Elmer Corporation, Physical Electronic Division. 1979.

9. J.A. Campbell, R.D. Smith, L.E. Davis, and K.L. Smith, "Characterization of micron-sized flyash particles by X-ray Photoelectron Spectroscopy (ESCA)," The Science of the Total Environment", 12, 75-85, (1979)

10. A.S. Damle, D.S. Ensor, and M.B. Ranade, "Coal combustion aerosol formation mechanisms: A Review", Aerosol Science and Technology 1, 119-133 (1982).

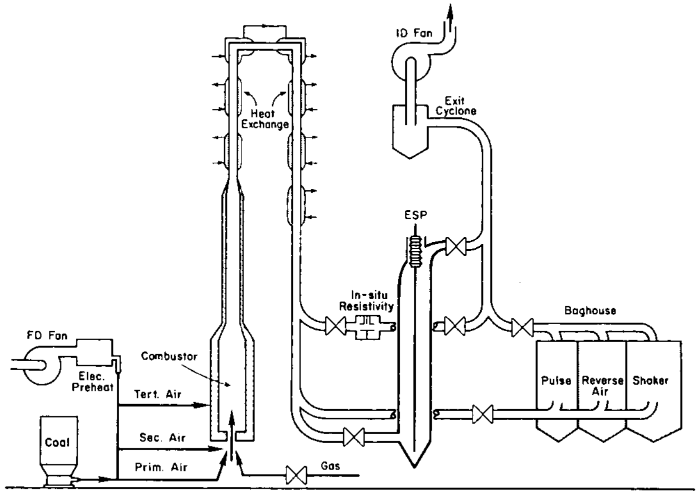

Figure 1. 34 kg/hr Coal Combustion Unit Employed for Ash Generation

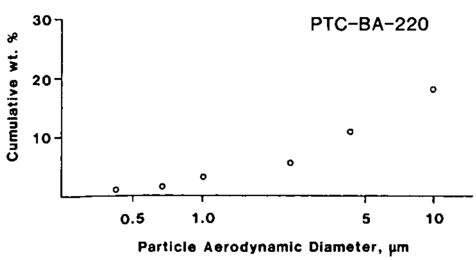

Figure 2. Baghouse Inlet Particle Size Distribution Determined with University of Washington's Mark III Cascade Impactor

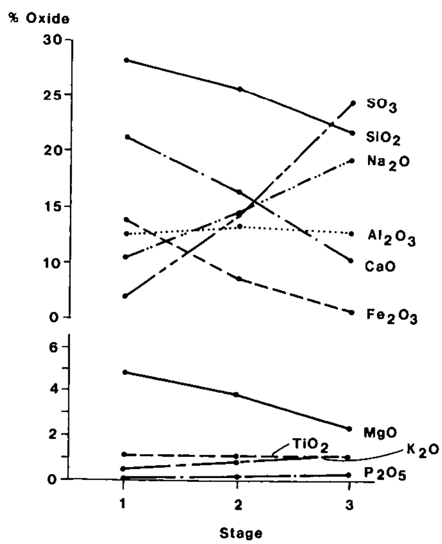

Figure 3. X-ray Fluorescence Analysis of Each Stage from the SASS Train Sampler

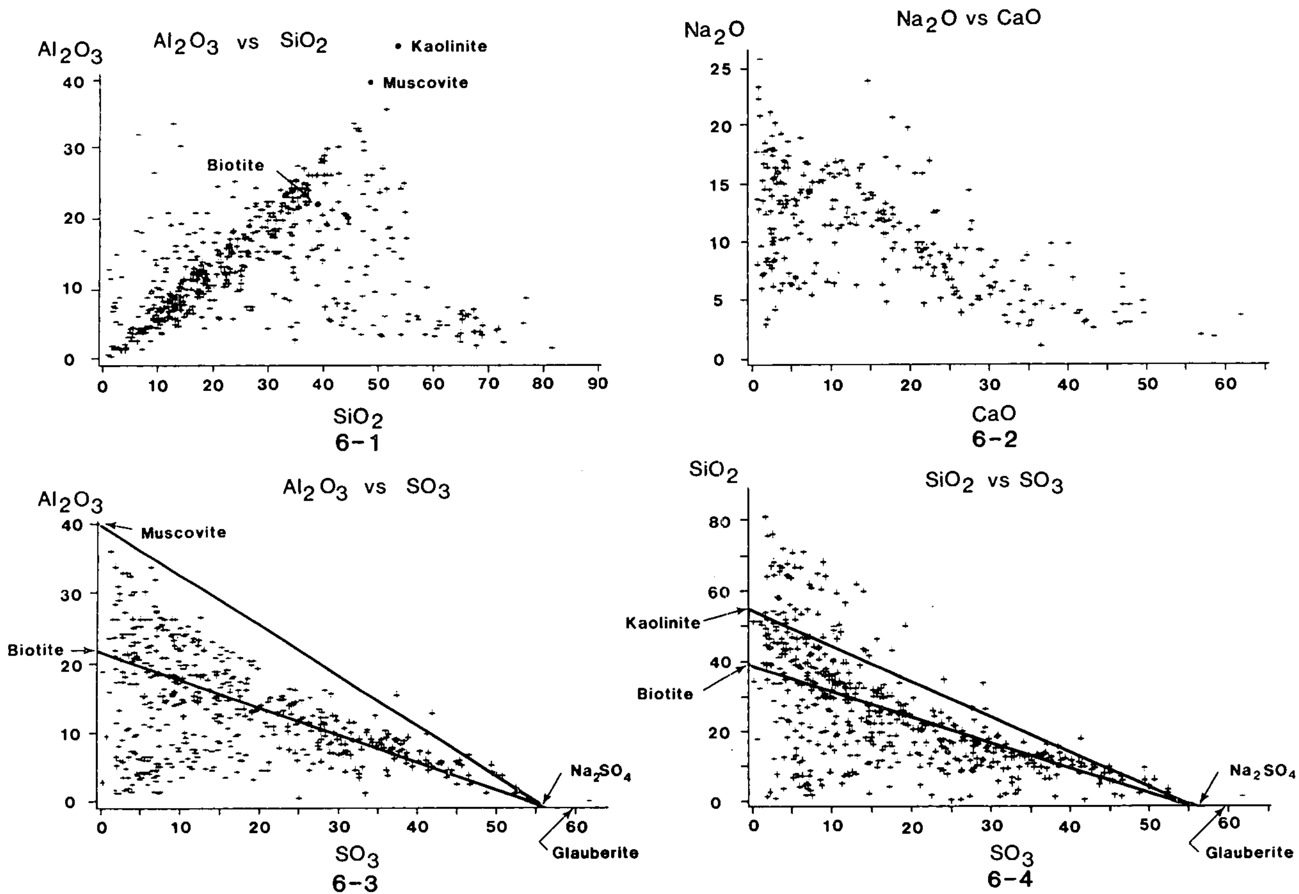

Figure 6. Compositional Relationships for SEM Data Combined from All Five Stages of the Multicyclone

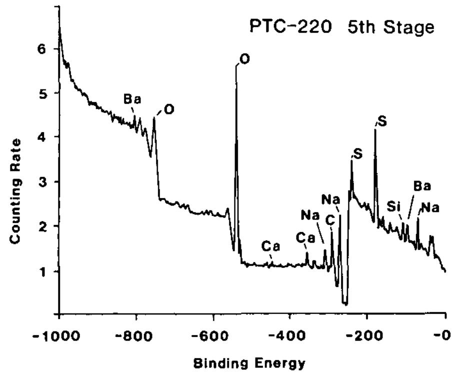

Figure 7. ESCA Scan of Stage 5 of the Multicyclone

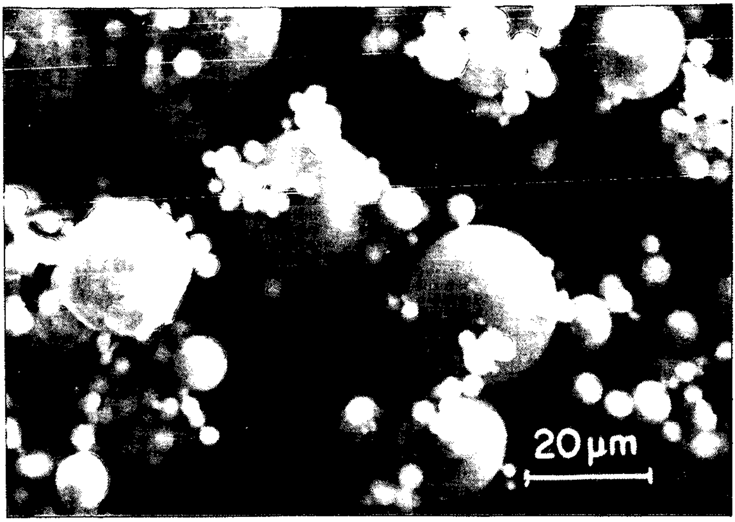

Figure 4. Secondary Electron Image of Particles from Stage 1 Multicyclone

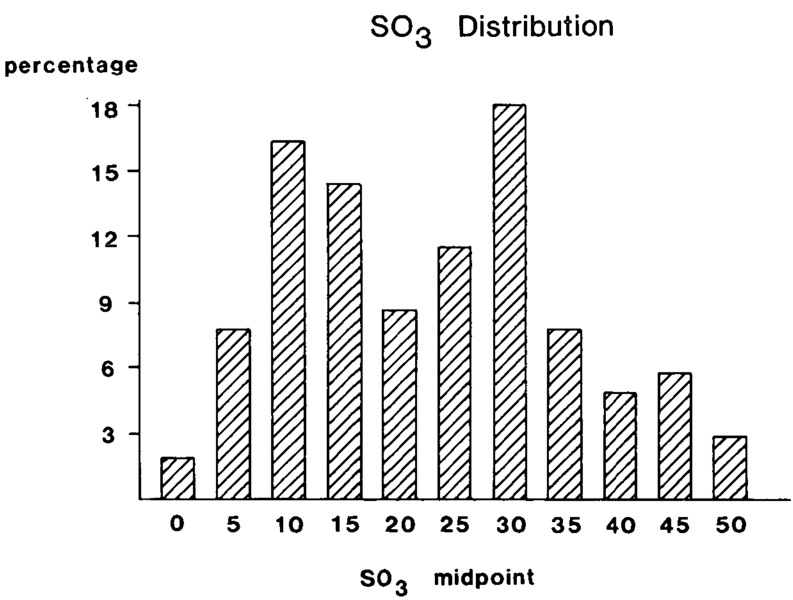

Figure 5. Concentration Population Distribution for SO_3 in Particles Collected in Stage 5 of the Multicyclone

On the Application of Complex Equilibrium Calculations to the Study of Mineral Matter during Coal Combustion

R. W. Carling, R. W. Mar, and A. S. Nagelberg

Sandia National Laboratories
Livermore, CA 94550

Introduction

Coal is a complex mixture of organic and inorganic materials. The inorganic portion, the mineral matter, usually makes up a significant portion of a coal's composition. The contents vary from seam-to-seam but can be as high as 32 weight percent, with an average of 15 weight percent for North American coals. Mineral matter acts as a diluent and is clearly undesirable in mining and transportation. It is also the cause of many problems within a combustor, such as gaseous and particulate emissions, fouling, slagging, corrosion, and erosion. With the increased usage of coal to fulfill the nation's and the world's energy requirements, higher mineral content coals will play a more significant role in the future. Therefore, it has become important to understand the behavior of the mineral matter and its consequences in coal utilization systems.

In this report we discuss the application of complex thermochemical calculations to the study of mineral matter behavior during the combustion of pulverized coal. In principle, one can specify the conditions of combustion (e.g., temperature, total pressure, and oxygen partial pressure) and then calculate the chemical equilibrium between reactions involving all or selected fractions of the elements found in a coal particle. These calculations may be used to predict the ash and gaseous species formed during combustion. Practical problems such as submicron fly ash formation, deposit formation, fouling, and corrosion may be addressed in this manner. An understanding of the formation of chemical species and the effects of changes in operating parameters and system chemistry on stability ranges should aid in identifying control strategies to combat harmful species. Basically, one is seeking to improve and control the thermochemical environment of the coal particle by the proper selection of operating parameters conditions and chemical constituents.

At the outset, one might question the application of equilibrium calculations to a nonequilibrium process such as coal combustion. There might not be time for chemical equilibrium to be attained, and this is particularly true where the reactants are large particulates. Equilibrium calculations should be considered an important first step, to be followed by an examination and incorporation of kinetic aspects. That is, educated guesses must be made concerning the reactivity and release of chemical constituents of the coal. Kinetic factors may be introduced by specifying the chemical state of the calculation, which may differ considerably from the total coal chemistry. Even if equilibrium conditions existed, uncertainties and variations in the calculated results may be introduced by a number of factors. In this paper we address the impact of three potential sources of error on mineral matter calculations, namely: 1) errors in the data, 2) selection of species, and 3) solution formation.

COMPLEX EQUILBRIUM CALCULATIONS

Numerous methods have been reported for computing complex thermodynamic equilibria, but all methods are based on the methods of Brinkley(1-2) or White, Johnson, and Dantzig(3). Brinkley's approach requires a formulation of independent chemical reactions and the simultaneous solution of equilibrium constant expressions. A superior approach, first suggested by White et al.(3), involves the computation of the composition that minimizes the Gibbs free energy of the system.

A number of independent computer programs to calculate complex equilibria by free energy minimization have been developed over the years(4-7). A major step forward was taken by Erickson(8-10) in his development of codes called SOLGAS and SOLGASMIX. These codes are capable of handling systems containing multiple condensed phases, ideal and nonideal solutions, and mixtures at constant total pressure and temperature. Bessman(11) modified SOLGASMIX to handle the additional case of equilibria at constant gas volume and variable pressure; his version is called SOLGASMIX-PV. Kee and Nagelberg(12) have taken SOLGASMIX-PV and interfaced it with CHEMKIN(13) that allows users at Sandia National Laboratories to share the vast thermochemical data base already available at Sandia.

While the equilibrium state of a complex chemical system is unique, there is no guarantee that all free energy minimization codes will provide the same answer. The Gibbs free energy surface may in fact consist of a number of local minima; thus, a free energy minimization routine could isolate on a local minimum rather than the grand minimum. Different numerical algorithms and convergence criteria selected for the iterative methods of free energy minimization and different programming structures may also lead to conflicting results. For example, Minkoff, Land, and Blander(14) have shown the NASA CEC code(4) to be incapable of converging on a solution when minor amounts of condensed phases are present in delicate balance. By using a primal geometric programming approach, Minkoff et al.(14) were able to eliminate convergence problems. Another cause of inaccurate results, perhaps the most obvious, is erroneous thermochemical data or poor data representation (curve fitting of the data).

A semianthracite coal composition obtained from the Penn State Coal Data Base (PSOC #627) was used in this study. The chemical composition of the coal is shown in Table I. A calculation was carried out in which this coal was reacted with 20 percent excess oxygen at a pressure of one atmosphere over a temperature range of 1000 to 2000 K. The species considered in the calculation are given in Table II. Thermochemical data for these species were taken from JANAF(15). The sodium-containing species predicted to form in the gas phase during combustion are shown in Figure 1. The major species were NaCl, NaOH, and Na, with NaOH dominating at high temperatures. Na_2SO_4 is predicted to form in lesser concentrations with a maximum peak at 1400 K. The condensed phases predicted to be present are shown in Figure 2. The principle condensed-phase species formed was SiO_2 at all temperatures. Below 1400 K, 2 mole percent Na_2SO_4 was observed as the only other phase. Above 1400 K, the sulfate was replaced by sodium silicate ($Na_2Si_2O_5$).

The purpose of the calculations described above is not to identify ash formation and deposit formation mechanisms; rather, we will use the results in Figures 1 and 2 as a baseline from which we will illustrate the effects of errors in the data, the number of species considered in the calculation, and solution effects.

EFFECTS OF VARIOUS CALCULATIONAL FACTORS

Errors in the Thermochemical Data

The quality of the thermochemical data used in calculations are often not evaluated when computational codes are used. Durie, Milne, and Smith(16) in their study of salt deposition from hydrocarbon flames, showed a change of only a few kcal/mol in the free energy of formation of a species resulted in a significant rearrangement in the relative proportions of deposited phases. However, one cannot generalize Durie's observations because the effect of a change in the free energy will vary from situation to situation, depending upon the number of chemical constituents, their thermodynamic stabilities, and their relative concentrations.

To illustrate the effect of errors in the data on coal combustion calculations, let us examine the sensitivity of the results to the free energy of Na_2SO_4. Figure 3 shows the predicted distribution of the sodium containing species in the gas phase if the free energy of Na_2SO_4 is reduced by 1 percent (1.2 kcal). It is seen that all curves exhibit the same qualitative behavior as those on Figure 1. In fact, except for the Na_2SO_4 curve, all species were virtually unaffected by the free energy change. The absolute amount of Na_2SO_4 is, of course, reduced.

The magnitude of the change is better illustrated in Figure 4, where the effect of varying the free energy by 1 and 5 percent is shown. In this illustration the situation appears to be buffered, and a drastic rearrangement of the relative proportions of all species does not result if the stability of just one species is modified. However, if one is

(15). Data for the rest of the minerals were taken from the work of Robie, Hemingway, Schafer, and Haas(17). The calculated gas phase composition is given in Figure 5, to be compared with that shown in Figure 1. It is seen that there is a major rearrangement of species, and as a whole, the species concentrations were all reduced by one to two orders of magnitude. Major changes also occured with the condensed phases, as seen in Figure 6. While SiO_2 remained as the primary condensed phase, Na_2SO_4 and $Na_2Si_2O_5$ were not stable. At temperatures between 1000 and 1220 K, the stable-condensed phases were SiO_2, pyrophyllite, and albite. At temperatures greater than 1220 K, the stable-condensed phases were silica, albite, and mullite. Thus, the results of complex equilibrium calculations can be significantly altered by the choice of species. Caution must be used when making the selection, and kinetic factors and exerimental information should be carefully evaluated.

Condensed Phase Solutions

Previous calculations pertaining to coal combustion have not allowed for the formation of condensed phase solutions. Solutions will obviously form when liquid silica, alkali silicates, and sulfates are present. The results on Figure 2 show that silica and sodium disilicate form, and the phase diagram information in the literature clearly suggest a solution will result(18). Let us now extend the baseline calculations on Figures 1 and 2 to include solution formation. For lack of better information, we will assume ideal solution behavior. The sodium-containing gas species formed in this case are shown in Figure 7. It is seen that the NaCl concentration is not affected, but noticeable changes in the behavior of NaOH, Na, and Na_2SO_4 is seen. While their concentrations maintain the same qualitative behavior, they all form in lesser amounts. Another way of representing the effects of solution formation is seen in Figure 8, where the ratio of concentration without solution formation to that where no solution is formed is shown.

SUMMARY

Complex equilibrium calculations may be a very useful tool in the study of mineral matter evolution in a coal combustor. Kinetic constraints must be applied but may be done within the context of equilibrium calculatons; kinetic considerations may be used to define a more realistic chemistry for the system. Equilibrium calculations are only an approximate representation of the real situation since not all possible chemical species can be considered in a calculation and the thermodynamic data for many species are uncertain. In order to utilize the results of complex calculations, one must understand the caveats and uncertainties created by these problems.

It has been shown that the qualitative behavior of chemical species is fairly insensitive to errors in the thermochemical data. However, the absolute concentrations of the species can change by orders of magnitude if the free concerned with absolute concentrations, great care must be taken to use accurate thermochemical data. A relatively small error of 1 kcal will change the concentration by a factor of two, and a change of two orders of magnitude is realized if a 5 kcal error in assumed. If the interest is in observing changes that occur as parameters are varied (i.e., the movement of phase boundaries), there is a smaller sensitivity to errors in the data.

Errors in data can also result from the misrepresentation of the data in the computer programs. Codes are generally constructed to be of generic use, and thus, a generalized approach to representing the data is used. For example, the NASA CEC code(4) and the Sandia code(12) use multiple-order polynomial fits over two-temperature ranges to represent the data. When dealing with complex condensed-phase mixtures, the free energies must be equal at transition temperatures. Failure to consider this constraint will result in an obvious error, such as a phase predicted to be present under conditions clearly out of its stability range (e.g., a solid phase predicted at temperatures above the melting point).

Species Considered in the Calculation

Complex equilibrium calculations are usually conducted with only a few species for several reasons. First and foremost, there are not many accurate self-consistent data. Also, calculations can become very time consuming, and the possibility of poor convergence behavior increases with the number of species, especially if many species are present in minor amounts(14).

When applying equilibrium calculations to the study of mineral matter behavior, one selects only a few species to consider by making assumptions concerning the reactive chemistry of the system. For example, aluminum is often found in coal but is usually not considered in the calculations because it is assumed to be present in kinetically and thermodynamically inert forms, such as alumino-silicates. If, however, Al is considered in the calculation, a significant change in the calculated results could occur.

To illustrate the point, let us repeat the equilibrium calculations of Figures 1 and 2, this time allowing the following aluminum-containing species to form:

gas phase: Al, AlO, Al_2O, $AlOH$, Al_2Cl_6

solid phase: Al_2O_3, $Al_6Si_2O_3$(mullite), $NaAlO_2$, $Al_2Si_2{}_9H_4$(kaolinite), $NaAlSi_2O_6$(jaedite), $Al_2Si_4O_{12}H_2$(pyrophyllite), Al_2SiO_5(kyanite), $NaAlSi_3O_8$(albite)

For our calculations, the thermochemical data for Al, AlO, Al_2O, $AlOH$, Al_2Cl_6, Al_2O_3, mullite, and $NaAlO_2$ were taken from JANAF energy of formation is varied by just a few percent. Failure to account for the formation of condensed phase solutions will also change the absolute concentrations substantially; however, the qualitative behavior is not affected as much. The qualitative and quantitative behavior of product species can be strongly influenced by the selection of species to be considered in the calculation.

References

1. S. R. Brinkley, Jr., J. Chem. Phys., 14, 563 (1946).

2. S. R. Brinkley, Jr., J. Chem. Phys., 15, 107 (1947).

3. W. B. White, W. M. Johnson, and G. B. Dantzig, J. Chem. Phys., 28, 751 (1958).

4. S. Gordon and B. J. McBride, "Computer Program for Calculation of Complex Chemical Equilibrium Compositions, Rocket Performance, Incident and Reflected Shocks, and Chapman-Jonquet Detonations", NASA SP273, NASA-Lewis Research Center, 1971.

5. D. R. Cruise, J. Phys. Chem., 68, 3797 (1964).

6. B. Sundman, CALPHAD Conference XI, Argonne National Laboratory, May 1982.

7. H. B. Levine, JAYCOR, San Diego, CA (Private Communication).

8. G. Erickson, Acta. Chem. Scand., 25, 2651 (1971).

9. G. Erickson and E. Rosen, Chemica Scripta, 4, 193 (1973).

10. G. Erickson, Chemica Scripta, 8, 100 (1975).

11. T. M. Bessman, "SOLGASMIX-PV, a Computer Program to Calculate Equilibrium Relationships in Complex Chemical Systems", ORNL/TM-5775, Oak Ridge National Laboratory, 1977.

12. R. J. Kee and A. S. Nagelberg, Sandia National Laboratories, Livermore, CA (Private Communication).

13. R. J. Kee, J. A. Miller, T. H. Jefferson "CHEMKIN: A General Purpose, Problem-Independent, Transportable, Fortran Chemical Kinetics Code Package", SAND80-8003, Sandia National Laboratories, 1980.

14. M. Minkoff, R. H. Land and M. Blander, CALPHAD Conference XI, Argonne National Laboratory, May 1982.

15. JANAF Thermochemical Tables 2nd edition, D. R. Stull and H. Prophet, eds., U. S. Department of Commerce, National Bureau of Standards, NSRDS-NBS 37, 1971.

16. R. A. Durie, J. W. Milne, and M. Y. Smith, Combust. Flame, 30, 221 (1977).

17. R. A. Robie, b. S. Hemingway, C. M. Schafer, and J. L. Haas, Jr., "Heat Capacity Equations for Minerals at High Temperatures", U. S. Geological Survey Rep. 78-934, U.S. Department of the Interior, 1978.

18. E. M. Levine, C. R. Robbins, and H. F. McMurdie, Phase Diagram for Ceramists (The American Ceramic Society, Columbus, Ohio, 1964).

19. L. J. Wibberley and T. F. Wall, J. Inst. Fuel, 61, 87 (1982).

20. W. D. Halstead and E. Raask, J. Inst. Fuel, 42, 344 (1969).

21. R. M. Allen and J. B. VanderSande, "Analysis of Sub-Micron Mineral Matter in Coal via Scanning Transmission Electron Microscopy", SAND82-8677, Sandia National Laboratories, Livermore, CA, 1982.

TABLE I

Chemical analysis of Pennsylvania #2 seam semianthracite coal (PSOC #627, provided by Pennsylvania State coal data base)

Elemental Analysis (dry)		Analysis of HTA dry coal	
77.08%	carbon	68.50%	SiO_2
2.61	hydrogen	22.80	Al_2O_3
.73	nitrogen	2.93	TiO_2
.52	organic sulfur	2.55	Fe_2O_3
.39	oxygen	.31	MgO
.01	chlorine	.33	CaO
18.67	mineral matter	.16	Na_2O
		1.66	K_2O
		.06	P_2O_5
		.25	SO_3

TABLE II

Chemical Species Considered in Complex Equilibrium Calculations

Gaseous Species: CO, CO_2, Cl, Cl_2, ClO, H, H_2, H_2O, HCl, H_2S, Na, Na_2, NaCl, Na_2Cl_2, NaH, NaOH, Na_2SO_4, O, O_2, OH, S, S_2, SO, SO_2, SO_3, SiO, SiO_2, SiS

Condensed Species: C, NaCl, NaOH, Na_2O, Na_2S, Na_2SO_4, Na_2SiO_3, $Na_2Si_2O_5$, SiO_2, SiC, Si

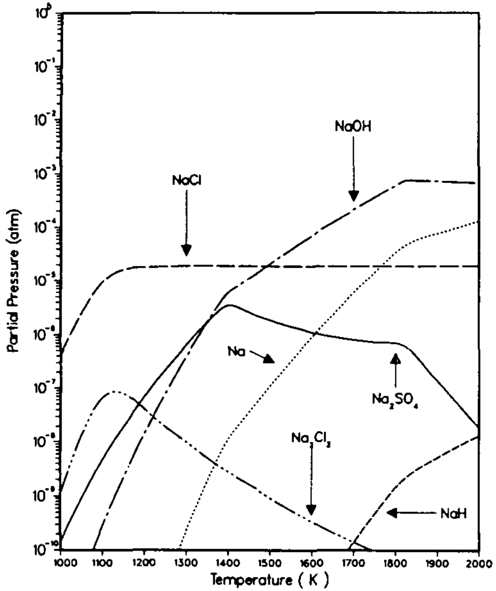

Figure 1. Sodium containing gas species predicted to form upon combustion of semianthracite Pennsylvania Seam #2 coal (PSOC #627) in 20% excess oxygen at various combustion temperatures. Chemical species considered in the calculation are given in Table I.

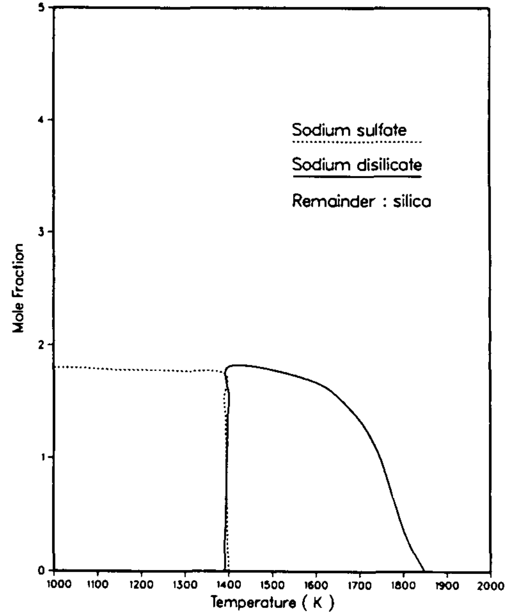

Figure 2. Condensed phases predicted to form upon the combustion of semianthracite Pennsylvania Seam #2 coal (PSOC #627) in 20% excess oxygen at various combustion temperatures.

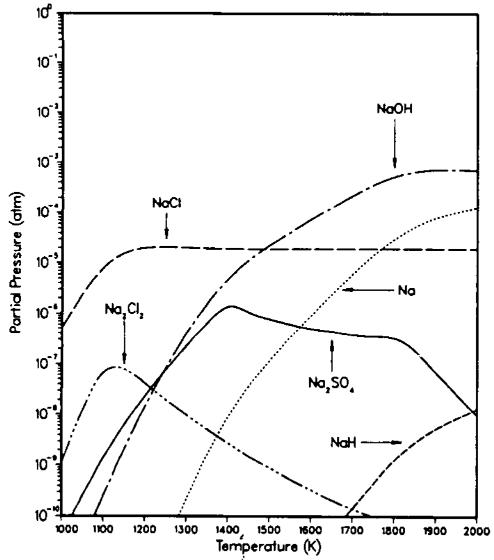

Figure 3. The effect of reducing the free energy of Na_2SO_4 by 1 percent. This distribution of gas species is to be compared with Figure 1.

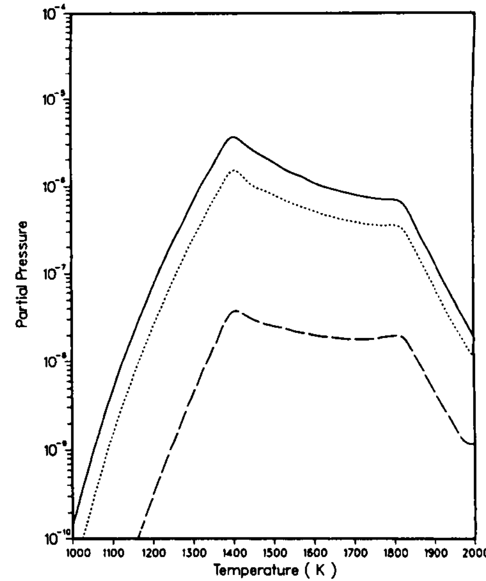

Figure 4. The effect of varying the free energy of Na_2SO_4; solid line - JANAF data, dotted line - less stable by 1 percent, dashed line - less stable by 5 percent.

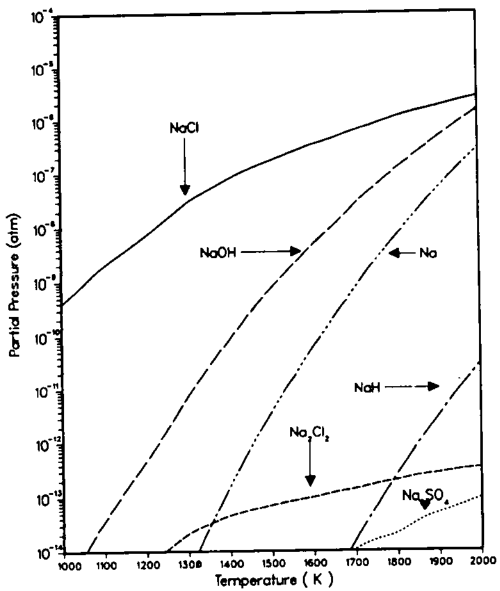

Figure 5. The effect of considering aluminum containing species in the calculations. This distribution is to be compared with that shown on Figure 1.

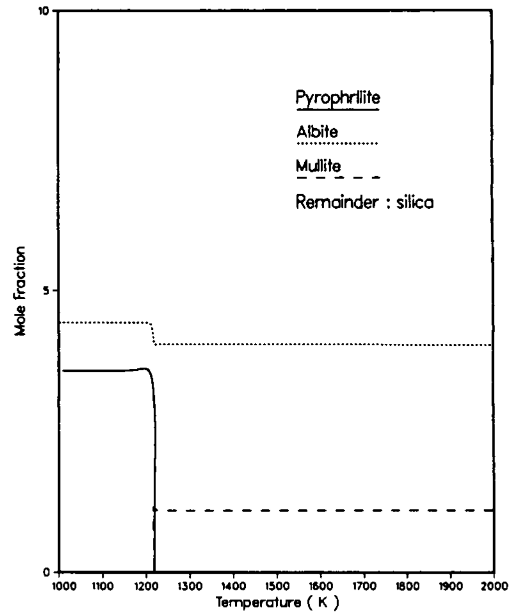

Figure 6. The effect of considering aluminum containing species in the calculations on the condensed phase distribution. This figure is to be contrasted with Figure 2.

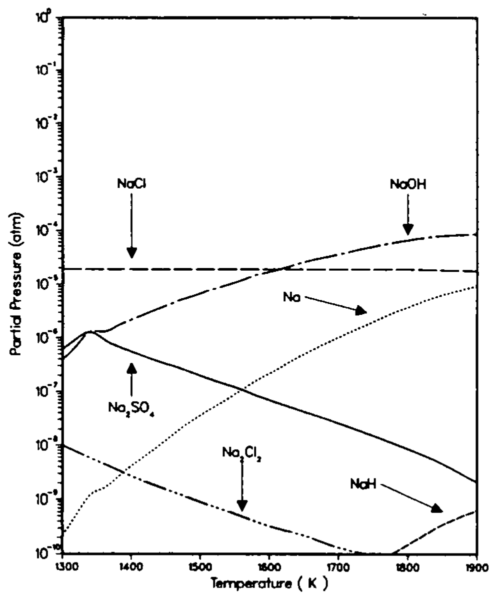

Figure 7. The effects of liquid solution formation between silica and sodium disilicate. This figure is to be compared with Figure 1.

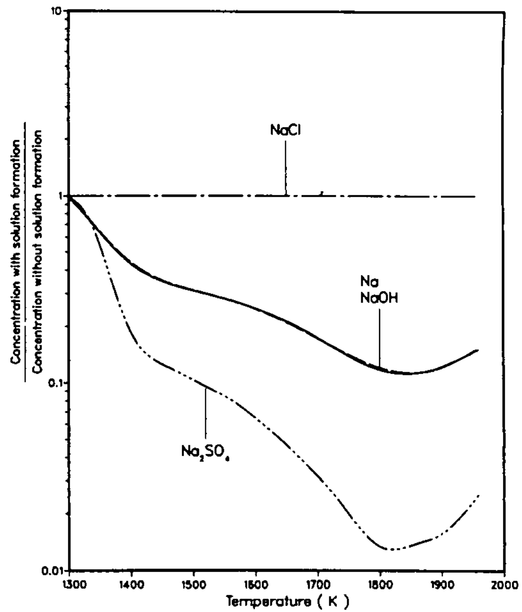

Figure 8. The effect of liquid solution formation between silica and sodium disilicate on the concentrations of species in the gas phase.

COMPARISON OF INORGANICS IN THREE LOW-RANK COALS

S. A. Benson

Grand Forks Energy Technology Center
U.S. Department of Energy
Grand Forks, N.D. 58202

P. L. Holm

University of Minnesota
Crookston, MN 56716

INTRODUCTION

In the use of low-rank coals it has been found that inorganic materials present in these coals can have adverse effects on process performance. During combustion processes some inorganics are liberated and react with other inorganics causing combustor fouling problems (1). The unique characteristics of the flyash produced upon combustion, frequently, if concentrations of sodium and sulfur are low, produces a high resisitivity ash making it difficult to collect in an electrostatic precipitator (2). In fluidized bed combustion, the inorganics of some low-rank coals can be used for sulfur retention (3) but bed agglomeration is a problem with high concentrations of sodium (4). In coal conversion processes the inorganic material can serve either as catalysts or catalyst poisons.

The occurrence of inorganic materials in low-rank coals is very complex. They are present as discrete mineral phases, as ions held by ion pair bonding with carboxyl groups or clays, and as coordinated metal ions. Knowledge of the distribution of inorganics within the coal could be used to predict effects in a given process.

We have chosen to compare the way in which inorganic material is found in three coals. These coals are two lignites from the Beulah mine, North Dakota, and the Bryan Mine, Texas and one subbituminous coal from the Rosebud mine, Montana.

EXPERIMENTAL

The coals were treated using a method modified from the procedure reported by Miller and Given (5). Figure 1 shows a flow sheet of the procedure used to examine the various coals. Each coal was ground to approximately 400 mesh in an alumina grinding apparatus. The ground coal was dried using a freeze drier. Analysis of the dried coal was performed using x-ray fluorescence (XRF) and neutron activation analysis (NAA). Duplicate samples were run by placing 15-20 g of coal in a plastic beaker with 100 ml of 1M ammonium acetate. This was heated to about 70°C and stirred for 20 hours. The sample was filtered, the residue washed and dried. The solution was transferred to a 500 ml volumetric flask and made up to volume.

The solution was analyzed by inductively coupled argon plasma spectroscopy (ICAP). Samples of the residue were analyzed by XRF and NAA. The residue was treated a second time with ammonium acetate followed by two 1M hydrochloric acid extractions using the same procedure as ammonium acetate extraction.

XRF analyses were performed using the energy-dispersive Kevex* 0700 subsystem. ICAP analysis were obtained using a Jarrell-Ash Mark I Model 975* multi-element analyzer. Analysis is controlled by a computer using a program for 22 elements. Neutron activation analysis used in this study was performed at North Carolina State University. The system and procedures have been described elsewhere (6).

RESULTS:

The table following shows the initial analysis of the three coals under consideration.

TABLE I

INITIAL ANALYSIS OF COALS, PARTS PER MILLION

Analysis	Beulah N.D. Lignite	Bryan Texas Lignite	Rosebud Montana Sub-bituminous
Al	3940	12360	3370
Ba	630	190	190
Ca	12800	7130	3520
Cr	3	21	4
Cu	22	24	30
Fe	5000	20950	8450
K	930	1970	120
Mg	2490	2000	920
Mn	58	300	35
Na	4340	310	87
Ni	22	40	52
Sr	485	80	90
Ti	185	1410	280
Ash	9.5%	24.5%	4.9%

These are followed by the anaylses obtained after the samples had been extracted twice with ammonium acetate. Table II shows the amount extracted from the original coal and the percent of the original.

Table III contains the results of the samples which have been extracted twice by hydrochloric acid. The amount extracted and the percent of the original coal are given.

DISCUSSION

Examination of the initial analysis reveals the dramatic differences in the amounts of inorganic material between the three coals. Aluminum, iron, potassium, and titanium are very high in the Bryan coal compared to the values for the Beulah and Rosebud coals. In general, the Bryan has a much high inorganic content which

*Reference to specific brand names does not imply endorsement by the U.S. Department of Energy.

TABLE II

ANALYSIS OF COALS AFTER EXTRACTION WITH AMMONIUM ACETATE

Analysis	Beulah PPM Extracted	Beulah % Extracted	Bryan PPM Extracted	Bryan % Extracted	Rosebud PPM Extracted	Rosebud % Extracted
Al						< 1
Ba	239	38	53	28	57	30
Ca	9728	76	442	62	2003	56
Cr			3	14		
Cu						
Fe						< 1
K	186	20	177	9	2	2
Mg	2241	90	1880	94	598	65
Mn	17	30	129	43	7	20
Na	3645	84	232	75	70	81
Ni						
Sr	422	87	65	81	22	90
Ti						
Ash remaining		4.9		23.8		3.8

TABLE III

ANALYSIS OF COALS AFTER EXTRACTION WITH HYDROCHLORIC ACID

Analysis	Beulah PPM Extracted	Beulah % Extracted	Bryan PPM Extracted	Bryan % Extracted	Rosebud PPM Extracted	Rosebud % Extracted
Al	2750	70	2719	22	1213	36
Ba	378	60	104	55	116	61
Ca	2688	21	1283	18	1408	40
Cr	1.5	51	9	41	1.5	37
Cu	21	90	10	76	5	18
Fe	1950	39	14246	68	5154	61
K			157	8	24	20
Mg	100	4	120	6	257	28
Mn	40	70	153	51	24	70
Na	43	1	9	3	10	12
Ni	6	27	21	52	3	5
Sr	63	13	15	19	56	63
Ti	22	12	409	29	154	55
Ash remaining		1.2		22.6		2.8

can also be seen by referring to the ash content listed in Table I. Further note should be taken of the high sodium content for the Beulah coal and related combustion problems (1).

The ammonium acetate extraction removes those inorganics associated as ions held by ion pair bonds to the carboxyl groups or to the clay minerals. The result of this extraction procedure is summarized in Table 2. For Beulah lignite most of the Ca, Na, Mg and Sr are bound to the carboxyl groups or possibly with the clays. The Bryan and Rosebud coals show similar trends for Ca, Na, and Sr. On the other hand, the Mg in Rosebud indicates a different association in the coal.

The hydrochloric acid extractions remove those species present in the coals as oxides, carbonate minerals, and coordinated metal ions. Larger discrepancies were noted between the coals extracted with HCl than ammonium acetate extracted. The fact that 70% of the Al is removed from Beulah is possibly explained by it being removed from the clay materials (7) but this is not well understood. Of particular interest is the removal of Ca, Mg and Sr in the Rosebud, which suggest that these elements were present as carbonate minerals. This relationship has also been suggested by Finkelman (8). The Fe is present in the coals as possibly a carbonate (siderite), oxide, and pyrite.

The changes in percent ash determined in the coal, after the ammonium acetate and HCl extractions reveal large changes in the amount of ash in Beulah and Rosebud. The total amount of inorganics removed by the ammonium acetate of the Beulah is approximately 48%. The percentage of ash removed for Rosebud was approximately 22% with ammonium acetate. The Bryan lignite has only 3% of its ash associated with the ion exchangeable fraction. The major inorganic constituents remaining in the coals after both extractions consist of quartz, clays and pyrite.

CONCLUSIONS

The alkaline and alkaline earth metals in all three coals are partially or totally removed with ammonium acetate extraction. The major differences between the coals are:

1. 48% of the total inorganics of the Beulah are removed with ammonium acetate by far the highest of 3 coals.

2. Bryan Texas lignite consists of mostly extraneous mineral matter including clays and quartz minerals (9).

3. The Rosebud subbituminous has higher percentages of Mg, Ca, and Sr associated as carbonates, revealed in the HCl extractions.

REFERENCES

1. D.K. Rindt, M.L. Jones, and H.H. Schobert. Investigations of the mechanism of ash fouling in low-rank coal combustion, Preceeding of the Engineering Foundation Conference, Henniker, NH, July 12-17, 1981

2. S.J. Selle, L.L. Hess, and E.A. Sondreal. Western fly ash composition as an indicator of resistivity and pilot ESP removal efficiency. Paper No. 75-02.5. Presented at 1975 Meeting, Air Pollution Control Association, Boston, MA, June 15-20, 1975.

3. G.M. Goblirsch, and E.A. Sondreal. Low-rank coal atmospheric fluidized-bed combustion technology. Proceedings, Technology and Use of Lignite, BuMines-Univ. of N. Dak. Symposium, Grand Forks, N. Dak., May 30-31, 1979, GFETC/IC-79/1, pp. 75-107.

4. S.A. Benson, F.R. Karner, G.M. Goblirsch, D.W. Brekke. Bed agglomerates formed by atmospheric fluidized bed combustion of a North Dakota lignite. ACS, Div. of Fuel Chem. Preprints, 27, No. 1, 174(1982).

5. R.N. Miller, and P.H. Given. Variations in inorganic constituents of some low-rank coals. in R.W. Bryers. Ash deposits and corrosion due to impurities in combustion gases. Hemisphere Publishing Corp., Washington, D.C. 1977. pp 39-50.

6. J.N. Weaver in Analytical Methods for Coal and Coal products, Vol I p. 377-401. Ed. Academic Press, Inc. N.Y. (1978).

7. R.N. Miller and P.H. Given. A geochemical study of the inorganic constituents in some low-rank coals. U.S. DOE report FE-2494-TR-1 (1979)

8. R.B. Finkelman in Atomic and Nuclear Methods in Fossil Energy Research p. 146-150 141, Plenum Press, New York and London, 1982

9. Energy Resources Co. Inc., Walnut Creek, CA 94596. Low-rank Coal Study, National Needs for Resource Development-Resource Characterization. DOE/FC/10066-T1 (Vol. 2) Nov. 1980, p 95-109

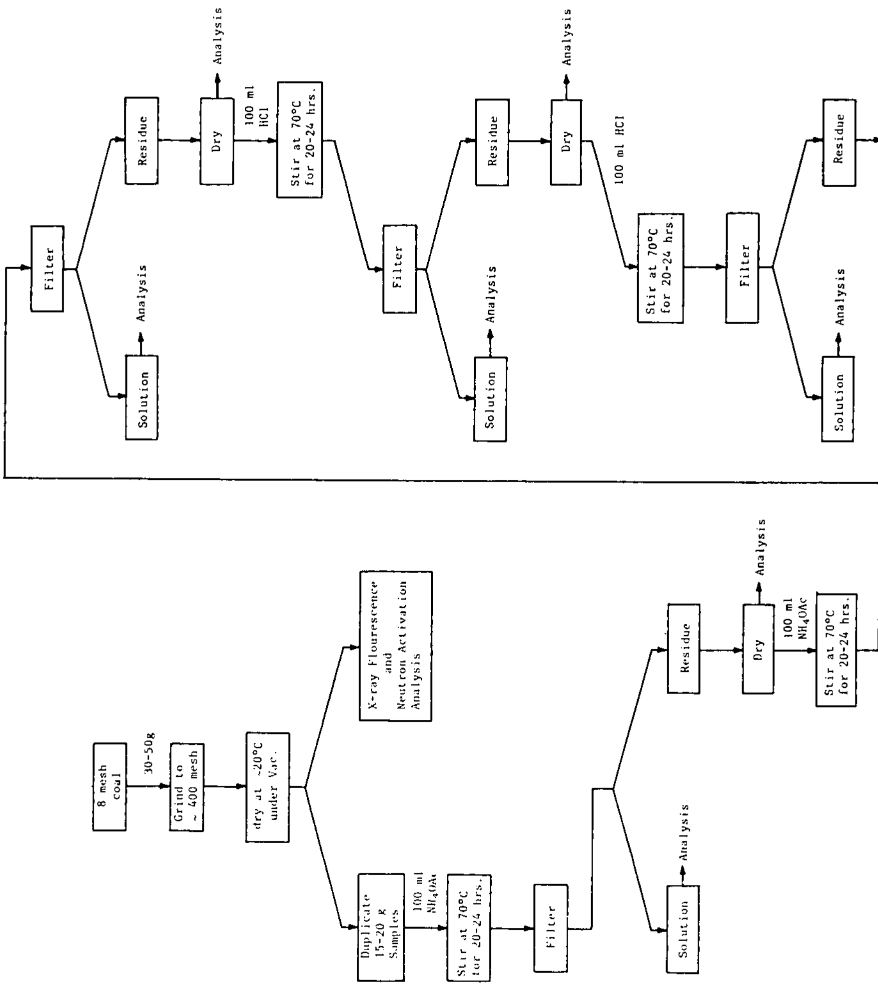

FIGURE 1. Flow diagram of extraction procedure.

Thermodynamics of Coal Chars; Correlation of Heat Capacity with Composition and Pyrolysis Conditions

Leslie L. Isaacs
Elliot Fisher

Department of Chemical Engineering
The City College of CUNY
140th Street and Convent Avenue
New York, NY 10031

Introduction

Heat capacity data for a char can be used to calculate the variation of the thermodynamic properties, H, S, G, etc. with temperature. Factors which affect the heat capacity are:

- o the rank and inorganic matter content of the parent coal;
- o the gaseous atmosphere present during pyrolysis;
- o the thermal history of the char.

Thermal history for a char is determined by:

- o the pyrolysis temperature;
- o the rate at which the coal temperature is raised from the ambient to the pyrolysis temperature;
- o the residence time of the char at the pyrolysis temperature.

The thermodynamic literature (1-5) for chars usually covers only limited temperature ranges and the thermal histories and compositions of the char samples are ill-defined or unavailable. The additivity approach (6,7) is usually employed to correlate the heat capacities in terms of char constituents; organic matter, ash and moisture.

In the thesis work of Wang (8) the effect and relative importance of the factors listed was assessed using a selected set of chars. Experimental data was collected between 80^{o}K and 300^{o}K. It was found that the heat capacities could be correlated with compositions and pyrolysis temperatures using a modified form of the Debye model for heat capacities (9). The correlation is in the form of an expression for an effective Debye temperature, $\theta(Tr)$:

$$\theta(Tr) = \theta_o(Tr)\ \exp[I(Tr)/x(1-x)] \qquad 1)$$

where Tr is a reduced temperature defined as:

$$Tr = T(K)/T_{pyrolysis}\ (K)$$

1-x = the atomic fraction of carbon in the ash free dry char.

$\theta_o(Tr)$ = a Debye temperature at Tr for a hypothetical char containing carbon atoms only.

$I(Tr)$ = an interaction parameter between the carbon atoms and the "other" atoms in the char.

θ_o and I were found by empirical fitting of the data for each family of chars. A char family consists of all the chars prepared from the same coal with one hour residence time.

Our present objective is to:

- o Test the limits of applicability of Equation 1 as an extrapolating function to calculate heat capacities of chars;
- o To refine the correlation model;
- o To factor into the correlating the effect of residence time at pyrolysis temperature.

Experimental Technique

The suite of samples from Wang's work was used for heat capacity measurements between 300°K and 900°K. The data were obtained using the differential scanning calorimetry (DSC) technique. Instrumentation consisted of a Dupont model 910 scanning calorimeter and a Dupont model 1090 thermal analyzer system. Sample heat capacities were calculated using the measured heat capacity of Sapphire as a standard for comparison.

Results

Typical experimental information obtained is illustrated in the following figures.

Effect of Pyrolysis Temperature

In Figure 1 we show DSC scans for two chars prepared from demineralized Virginia Coal (PSOC-265). The results show that the heat capacity of the chars increase with temperature between 300K and 900K. Also the char prepared at 1100°C has a higher heat capacity at any given temperature (over the range) than the 700°C char. For quantitative comparison the heat capacities need to be normalized. The normalizing procedure is arbitrary. We have elected to normalize all our data to the number of atoms in the ash free char.

Effect of Residence Time

In Figure 2 we show DSC scans for chars prepared from demineralized Virginia coal at 1100°C pyrolysis temperature.

The chars differ in their thermal history by the length of their residence time at pyrolysis temperature. The normalized heat capacities at a given temperature vary in magnitude with the residence time.

A minimum in heat capacity is seen to occur if the data is replotted as heat capacity versus residence time. From the present data the minimum is around two hours residence time. Our interpretation of this phenomenon is that two separate events are being observed. One is the equilibration of the chemical composition at 1100°C by breakage of C-H bonds. The smaller the number of such bonds in the char the smaller is its heat capacity. The second is the approach of the char to structural equilibrium by solid state diffusion. The char is graphitizing with an apparent increase in heat capacity.

Effect of Retained Inorganic Matter

In Figure 3 the DSC scans of chars prepared at 700°C with one hour residence time are compared. Both of these chars were prepared from Virginia coal. However, in one case the coal was demineralized using the acid wash procedure prior to pyrolysis. On a per gram sample basis the heat capacity of the mineral matter containing char is about 40 to 80% higher than the demineralized char. The inorganic matter heat capacity is additive to the organic matter heat capacity.

Conclusions

At the time of preparation of this preliminary paper (December 1982) the calculation for testing and refining the correlation model have not been completed. We expect to be able to present them at the meeting.

References

1. Delhaes, P., and Y. Hishiyama. Carbon 8:31 (1970).
2. Kamiya, K., S. Mrosowski and A.S. Vagh. Carbon 10:267 (1972).
3. "Thermal Data on Gasifier from Synthane Test," Internal Report, Thermodynamics Research Group, Department of Energy, Bartlesville Energy Research Center (1973).
4. Kasatochkin, V.I., K. Usenbaev, V.M. Zhadanov, K. Sabyraliev, M. Rasalhaev and E. Zhumalieva. Dokl. Akad. Nauk (USSR), 216:93 (1974).
5. Tye, R.P., Desjarlais, A.O., Singer, J.M., High Temper - High Pressures, 13:57 (1981).
6. Kirov, N.Y. Brit. Coal Util. Res. Assoc. Mon. Bull. 29 (1965), p. 33.

References (cont.)

7. Eisermann, W., P. Johnson and W.L. Conger. Fuel Proc. Technol. 3:39 (1980).
8. Isaacs, L.L. and Wang, W.Y. in "Chemical Engineering Thermodynamics." S.A. Newman, Ed. (Ann Arbor Science 1982) pps. 451-459.
9. Maradudin, A.A. in "Solid State Physics" (Academic Press, 1966) 18: p. 274.

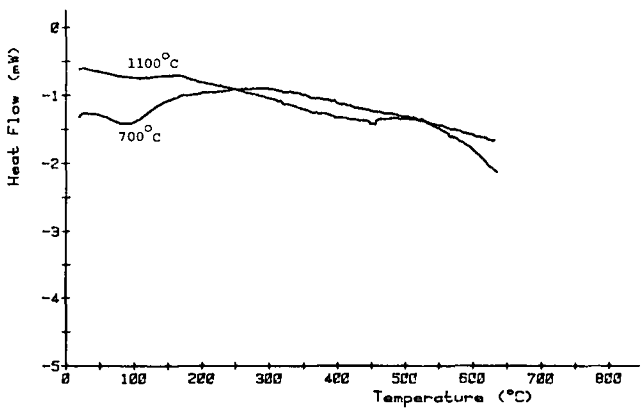

Figure 1. DSC Scans on Virginia Chars. (One hr. residence time - demineralized).

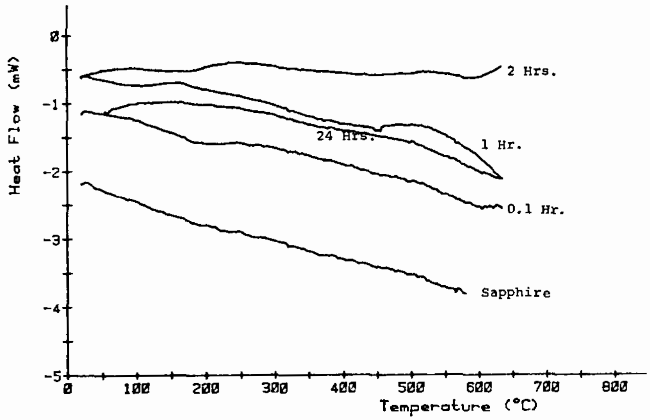

Figure 2. DSC Scans on Virginia chars. (1100°C Demineralized)

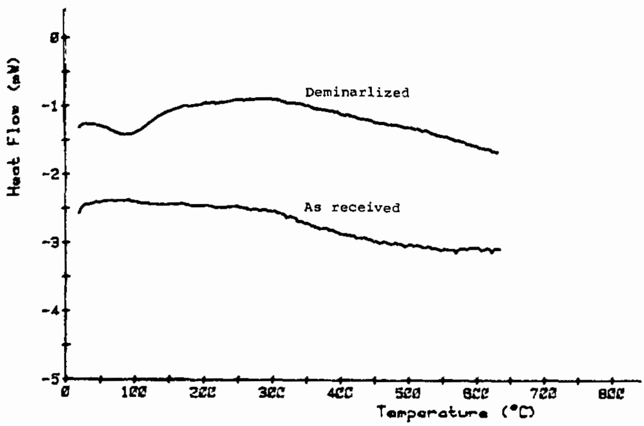

Figure 3. DSC Scans on Virginia chars. (700°C - One hour residence time)